IEEE Access
Multidisciplinary | Rapid Review | Open Access Journal

Received June 19, 2018, accepted July 31, 2018, date of publication August 6, 2018, date of current version August 28, 2018.

Digital Object Identifier 10.1109/ACCESS.2018.2863255

Low-Complexity and Robust Symbol Timing Synchronization Scheme for MIMO DVB-T2 Systems

YONG-AN JUNG[1], HYOUNG-KYU SONG[2], AND YOUNG-HWAN YOU[1]
[1]Department of Computer Engineering, Sejong University, Seoul 143-747, South Korea
[2]Department of Information and Communication Engineering, Sejong University, Seoul 143-747, South Korea

Corresponding author: Young-Hwan You (yhyou@sejong.ac.kr)

This work was supported by the Basic Science Research Program through the National Research Foundation of Korea funded by the Ministry of Education under Grant NRF-2018R1D1A1B07048819.

ABSTRACT The digital video broadcasting-terrestrial-second generation (DVB-T2) system provides the so-called P1 symbol as preamble for the fast synchronization tasks. In this paper, a simple and robust timing synchronization scheme for a multiple-input multiple-output orthogonal frequency-division multiplexing (MIMO–OFDM)-based DVB-T2 system is proposed to improve the initial time and frequency synchronization performance. In doing so, the proposed synchronization scheme utilizes a decimated correlation for the P1 symbol timing detection, thus producing a sharper peak timing detection metric. A new timing detection metric can help the proposed scheme to be robust against frequency-selective fading. It is found that the proposed synchronization scheme works well with a reduced computational complexity and outperforms the conventional estimation scheme.

INDEX TERMS DVB-T2, P1 symbol, orthogonal frequency division multiplexing, timing synchronization, MIMO-OFDM.

I. INTRODUCTION

Orthogonal frequency division multiplexing (OFDM) has been commonly used thanks to its capability to support high data rate and provide robustness regarding frequency-selective fading channels. As a promising technology, OFDM has been chosen for a variety of terrestrial digital multimedia broadcasting standards like digital audio broadcasting (DAB), digital radio mondiale (DRM), digital video broadcasting-terrestrial-second generation (DVB-T2), and DVB next generation handheld (DVB-NGH) [1]–[5]. The DVB-T2 has been standardized to aim at the delivery of interactive content that demands a high bandwidth, like high definition television (HDTV) and 3D TV [4]–[6]. For this purpose, the DVB-T2 standard has adopted the well-known multiple-input single-output (MISO) antenna technology [7]. The DVB-NGH system is known as the first broadcast standard to incorporate the multiple-input multiple-output (MIMO) concept as the primary technology to deal with increasing transmission capability without consuming no extra wireless bandwidth [8] Moreover, a number of standardization forums such as integrated services digital broadcasting (ISDB) and advanced television systems committee (ATSC) are adopting MIMO technology [9]–[11].

Since DVB-T2 utilizes OFDM modulation, it is of great significance to develop a reliable symbol timing offset (STO) and carrier frequency offset (CFO) estimation strategy under the scattered multi-path fading channel environments [12]. The problems of fast synchronization of STO and accurate estimation of CFO are of paramount importance to the OFDM-based broadcasting system, where the zapping time among channels is greatly affected by synchronization. If not accurately estimated and compensated, they introduce inter-carrier interference (ICI) or inter-symbol interference (ISI), which leads to severe performance degradation. For the purpose of mitigating the ICI and ISI effects, the receiver first has to acquire correct STO. Subsequently, it is inevitable that the CFO on the OFDM block is found and compensated for to combat the ICI. For the fast synchronization tasks, DVB-T2 has provided a specific symbol, the so-called P1 symbol, not only to discovery the existence of DVB-T2 signals but also to disclose the fundamental information on DVB-T2 system parameters for succeedingly decoding OFDM signals [4].

The DVB-T2 guidelines [12] recommend a strategy for robust time and frequency estimation even at a low signal-to-noise ratio (SNR). However, a trapezoidal-shaped timing detection metric may hinder accurate time and frequency synchronization. In order to reinforce the synchronization performance, many solutions have been developed [13]–[18]. One class of detection method focuses on producing spike-like correlation peak to improve its performance, leading to a more sophisticated estimation [13]–[15]. In [13], the timing detection metric is designed to be triangle-like shape, whereas the works in [14] and [15] propose the correlation with quadratic decaying neighboring points, which contributes to performance improvement. In [16] and [17], a two-stage timing synchronization approach is proposed to reduce the computational complexity. These improved algorithms still suffer from obvious performance loss, especially under low SNR conditions and frequency-selective fading channels. Hence, there is still room for a much better estimation algorithm, one that is immune to the fading impairment and is not computationally demanding.

In this paper, a simple and robust algorithm for joint estimation of the STO and CFO is proposed in a MIMO-OFDM DVB-T2 system. For this purpose, the correlation output is decimated for the timing detection metric to have a sharp peak with a reduced complexity. We demonstrate via simulations that the proposed detection scheme well works with affordable complexity and significantly outperforms conventional estimation scheme.

The remainder of this paper is structured as follows. Section II describes how the P1 symbol is built in the DVB-T2 specification and summarizes the synchronization process in DVB-T2. In Section III, we briefly revisit the conventional joint estimation of STO and CFO and present its extension to MIMO transmissions. A computationally efficient and robust joint estimation scheme is proposed in Section IV. Section V presents the simulation results that prove the usefulness of the proposed scheme. Conclusions are drawn in Section VI.

II. SYSTEM MODEL

In DVB-T2 system, a super frame is composed of a lot of T2-frames. The T2-frame always begins with a P1 symbol. The initial phase in synchronization, referred to as frame synchronization, aims to recognize the beginning of the T2-frame. For this purpose, DVB-T2 uses the P1 symbol as the dedicated pilot to aid the receiver to capture the T2 signal immediately instead of the entire T2-frame. In addition, the P1 symbol conveys a lot of fundamental transmission parameters (TPS) such as the fast Fourier transform (FFT) size, the SISO/MIMO mode, and presence of future extension frame (FEF) [4]. The P1 symbol also helps the receiver to accomplish fine time and frequency estimations. The P1 symbol is composed of an OFDM symbol with a length of $N_a = 1024$ subcarriers "A" and its two time domain (TD) repetitions, which are notated by "C" and "B", respectively. Two copies of the OFDM symbol with $N_a = 1024$ subcarriers are shifted by a fixed amount $f_s = 1/(N_a T_s)$ to build the guard interval (GI) of the P1 symbol, where T_s is the sampling period. The two GIs correspond the frequency-shifted duplicates of the first $N_1 = 542$ samples and the last $N_2 = 482$ samples of the main middle part of the P1 symbol, respectively. The TD signal to be transmitted at antenna l reads

$$x_l(n) = \sum_{k=0}^{N-1} X_l(k) e^{j2\pi kn/N}, \quad l = 1, 2, \cdots, N_t \tag{1}$$

where N is the FFT size, $X_l(k)$'s are the signal transmitted at the l-th transmit antenna in the frequency domain (FD), and N_t denotes the number of transmit antennas. The TD baseband signal of the P1 symbol can be expressed as

$$x_l(n) = \begin{cases} p_A(n) e^{j2\pi f_s n T_s}, & 0 \le n < N_1 \\ p_A(n - N_1), & N_1 \le n < N_1 + N_a \\ p_A(n - N_a) e^{j2\pi f_s n T_s}, & N_1 + N_a \le n < 2N_a \end{cases} \tag{2}$$

where $p_A(n)$ denotes the TD baseband expression of part "A" and f_s indicates the frequency shift used to both parts "B" and "C" to discriminate between the P1 symbol and the common GI.

In the frequency domain of "A", only 384 subcarriers carry signaling information, whereas others are suppressed to be null. The contents of the P1 symbol will be the same among the transmit antennas. Similar to other studies in [19]–[21], we consider the MIMO-OFDM system experiencing a single common CFO by assuming that there is one single oscillator used for frequency conversion, and the difference among CFOs at transmit-receive antenna couples is marginal. Therefore, the signal received at the receive antenna m is written as

$$y_m(n) = \sum_{l=1}^{N_t} x_l(n - \delta) e^{j2\pi \epsilon n/N} \otimes h_{lm}(n) + w_m(n), \ m = 1, 2, \cdots, N_r \tag{3}$$

where $\otimes$ stands for linear convolution operation, N_r is the number of receive antennas, δ is the unknown STO, ϵ is the CFO normalized by the bandwidth $1/T_s$, $h_{lm}(n)$ is the baseband equivalent discrete-time channel impulse response (CIR) from transmit antenna l to receive antenna m, and $w_m(n)$ denotes zero-mean complex Gaussian at the receive antenna m.

The overall procedure of the DVB-T2 synchronization is illustrated in Fig. 1. At the receiver, the synchronization processing primarily concentrates on performing time and frequency synchronization as well as decoding the TPS. The initial symbol timing estimation at the receiver is the first stage for precisely capturing the start of a frame, which intends to find the exact position of T2-frame. The goal of timing estimation during this phase is to be robust against the amount of CFO as well as lead to a impulse-like peak at the correct arrival of the preamble. After the initial timing acquisition process, it is unavoidable to achieve the fine STO and CFO synchronization, which can be performed in a sequential or a joint manner. After compensating the fractional CFO, part "A" of the P1 symbol is disclosed and

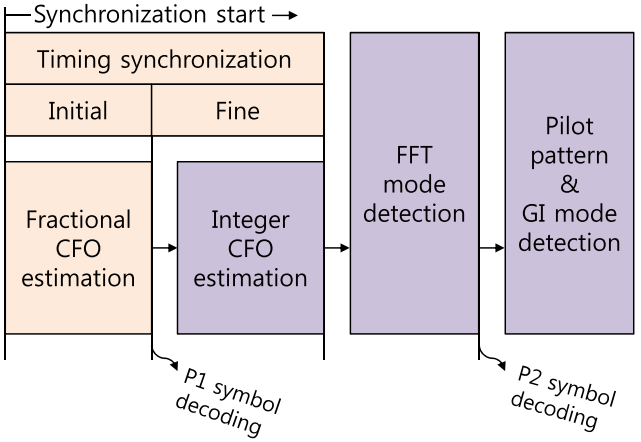

FIGURE 1. Synchronization process in DVB-T2.

translated to the FD for integer CFO estimation and signaling detection. Once the P1 symbol is decoded, the receiver has knowledge of the FFT size so that it can move forward to decide the GI, and the receiver has to detect the L1 signalling in P2 symbol. By decoding the L1 signalling information, the pilot pattern and GI mode can be detected. In this paper, we concentrate our attention on timing synchronization without being concerned about capturing the TPS.

III. CONVENTIONAL SYNCHRONIZATION SCHEME

We briefly present the correlation-based conventional synchronization scheme, which utilizes a double branch correlator running in parallel [12]–[15]. The P1 symbol can typically be detected by correlating the two replicas attached at either side of the main body of the P1 symbol. Referring to [12]–[15], the generalized block diagram of the correlation-based conventional P1 symbol detection schemes is shown in Fig. 2, where the operator D^x denotes the discrete time-shift operator by x times samples, and the upper and lower sliding correlators (SCs) are performed with duration of N_x and N_y, respectively. In Fig. 2, the upper branch is used to correlate parts "A" and "C", whereas the lower branch is for correlating parts "A" and "B". For the purpose of a simple derivation, it assumed that the frequency-shifted replicas have been already compensated for at the receiving side by multiplying them by $e^{-j2\pi f_s n T_s}$.

For timing and CFO estimation, the basic concept used in the context of SISO OFDM [12] can be immediately extended to the MIMO DVB-T2 system after making necessary modifications. In the MIMO configuration, the upper and lower sliding correlations in the m-th receive antenna, which are referred to as $B_m^1(g,\epsilon)$ and $B_m^2(g,\epsilon)$ respectively, can be written by

$$B_m^i(g,\epsilon) = \sum_{n=g}^{N_a-1+g} y_m(n) y_m^*(n+N_i), \quad i = 1,2, \quad m = 1,2,\cdots,N_r \tag{4}$$

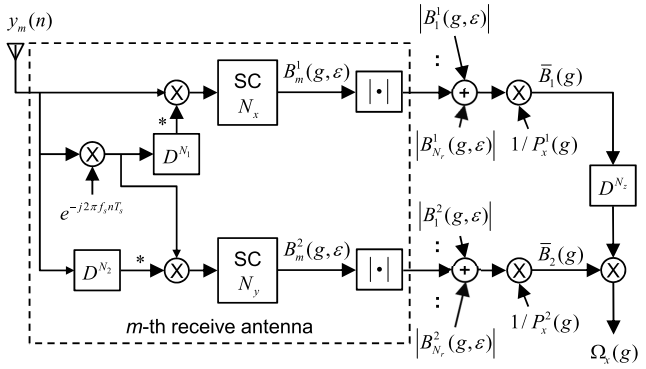

FIGURE 2. Block diagram of the correlation-based conventional P1 symbol detection scheme.

which is implemented by a sliding correlation of duration $N_x = N_y = N_a$. The power-normalized correlation using all the receive branches reads

$$\bar{B}_i(g) = \frac{1}{P_a^i(g)} \sum_{m=1}^{N_r} \left| B_m^i(g,\epsilon) \right|, \quad i = 1,2 \tag{5}$$

where $P_a^i(g)$ is the instantaneous power defined by

$$P_a^i(g) = \sum_{m=1}^{N_r} \sum_{n=g}^{N_a-1+g} |y_m(n+N_i)|^2, \quad i = 1,2. \tag{6}$$

In summary, the design parameters in Fig. 2 are set to $N_x = N_y = N_z = N_a$ and $P_x^i(g) = P_a^i(g)$ to implement the detection scheme [12]. Consequently, the timing detection metric can be calculated by time-alignment and multiplication of the two branches output as follows

$$\Omega_a(g) = \bar{B}_1(g - N_a)\bar{B}_2(g) \tag{7}$$

where $\bar{B}_1(g)$ and $\bar{B}_2(g)$ have a trapezoidal shape, which makes it difficult to achieve a sophisticated adjustment of the FFT window position in the presence of noise.

To solve this problem, a simple adaptation on the timing detection metric is made in [13]

$$\Omega_b(g) = \bar{B}_1(g - N_2)\bar{B}_2(g). \tag{8}$$

Referring to Fig. 2, similarly, one can see that $N_x = N_y = N_a$, $N_z = N_2$, and $P_x^i(g) = P_a^i(g)$ to implement (8). This configuration forces the double SCs to produce a triangular shaped pulse in (8). This timing detection metric eliminates the flat trapezoidal shape in (7) such that the time ambiguity can be resolved. There are still a few drawbacks to be overcome in (8). One of them is a substantial performance degradation under multipath fading environments.

For the purpose of more impulse-like timing detection metric, the correlation output can be modified in [14] and [15], which takes expression

$$C_m^i(g,\epsilon) = \sum_{n=g}^{N_i-1+g} y_m(n) y_m^*(n+N_i), \quad i = 1,2, \quad m = 1,2,\cdots,N_r. \tag{9}$$

In this scheme, the power-normalized correlation is similarly expressed as

$$\bar{C}_i(g) = \frac{1}{P_c^i(g)} \sum_{m=1}^{N_r} \left| C_m^i(g, \epsilon) \right|, \quad i = 1, 2 \tag{10}$$

with

$$P_c^i(g) = \sum_{m=1}^{N_r} \sum_{n=g}^{N_i-1+g} |y_m(n + N_i)|^2, \quad i = 1, 2. \tag{11}$$

In this case, it is obvious from Fig. 2 that $N_x = N_1$, $N_y = N_2$, $N_z = 2N_2$, and $P_x^i(g) = P_c^i(g)$, and $B_m^i(g, \epsilon)$ and $\bar{B}_i(g)$ are replaced by $C_m^i(g, \epsilon)$ and $\bar{C}_i(g)$, respectively. Therefore, the timing detection metric can be modified to

$$\Omega_c(g) = \bar{C}_1(g - 2N_2)\bar{C}_2(g) \tag{12}$$

which makes the peak more distinct than (8) such that the need for an extra fine symbol timing estimation process is removed.

Since a sharp peak of the timing detection metric is seen at the exact symbol timing whereas the values are almost zeros at all other positions, by looking for the maximum of the timing detection metric, the coarse timing synchronization is performed as follows

$$\hat{\delta} = \arg \max_g \{\Omega_c(g)\}. \tag{13}$$

The estimation parameters are now decoupled and an estimate of ϵ is obtained by finding the angle of the accumulation of $C_m^i(\hat{\delta}, \epsilon)$ over all combinations of m's and i's in MIMO-OFDM systems. Assuming that all transmit-receive antenna couples undergo the same CFO [19]–[21], the CFO can be estimated to be

$$\hat{\epsilon} = \arg \left\{ \sum_{m=1}^{N_r} \sum_{i=1}^{2} C_m^i(\hat{\delta}, \epsilon) \right\} \tag{14}$$

where $\arg\{x\}$ returns the angle of a complex variable x.

IV. PROPOSED SYNCHRONIZATION SCHEME

In the synchronization process, the first step is to find the coarse symbol timing. The purpose of coarse synchronization is to detect a tentative estimate of the beginning of the preamble for the incoming T2-frame, which is considered as possible candidates that are further checked during the following phase in order to acquire the fine STO and CFO in a joint manner. The coarse symbol timing detection scheme performs to get the best estimate of δ employing the P1 symbol. This section presents the STO and CFO estimation scheme in the DVB-T2 system, which works well with a reduced computational complexity. To accomplish this, a joint time-frequency algorithm is devised with aid of the decimated correlation.

A. COARSE SYMBOL TIMING ESTIMATION

At the receiver, the decimated correlation is conducted over N_r receive branches to reinforce the performance under the multipath fading channel, which is performed on every N_r sample at each receive antenna. Similar to Fig. 2, the proposed scheme comprises two SCs: the upper branch relative to part "C" denoted by $D_m^1(g, \epsilon)$ and the lower branch relative to part "B" denoted by $D_m^2(g, \epsilon)$. The sliding correlation in the m-th receive antenna ($m = 1, 2, \cdots, N_r$) can be defined by

$$D_m^i(g, \epsilon) = \sum_{n=gN_r+m-1}^{N_i+gN_r+m-2} y_m(n) y_m^*(n + N_i), \quad i = 1, 2 \tag{15}$$

which indicates that the correlation outputs at each receive antenna are decimated by a factor of N_r. By lining up time scales, the overall correlation in the m-th receive antenna ($m = 1, 2, \cdots, N_r$) takes the form

$$\bar{D}_m(g) = \frac{1}{Q_m(g)} \left| D_m^1(g - 2N_2, \epsilon) + D_m^2(g, \epsilon) \right| \tag{16}$$

where $Q_m(g)$ is the instantaneous power at the m-th antenna given by

$$Q_m(g) = \sum_{i=1}^{2} \sum_{n=gN_r+m-1}^{N_i+gN_r+m-2} |y_m(n + N_i)|^2. \tag{17}$$

In the case of 2×2 MIMO configuration, $D_m^1(g, \epsilon)$ in (15) represents the decimated correlation between two parts "A" and "C", whereas $D_m^2(g, \epsilon)$ is the decimated correlation between parts "A" and "B". In our scheme, $D_m^i(g, \epsilon)$'s are respectively computed every two samples in accordance with (15). Therefore, the number of uncorrelated samples with the respective part of P1 symbol becomes twice within the correlation window in comparison with (9). As a consequence, the incline of each correlation output steeply decreases after its true correlation peak.

After aligning the time scales and collecting the output of the N_r receive branches, we formulate the timing detection metric as

$$\Omega_p(g) = \sum_{m=1}^{N_r} \bar{D}_m(g + m - N_r). \tag{18}$$

Notice that (16) allows (18) to be independent of CFO. Finally, the arrival timing of an incoming T2-frame is detected by

$$\hat{\delta} = \arg \max_g \left\{ \Omega_p(g) \right\} \tag{19}$$

which only informs us of the arrival of a new symbol, without saying its exact beginning position. Hence, a sophisticated fine timing estimation procedure needs to be performed.

The normalized timing detection metric versus SNR is depicted in Fig. 3 when 2×2 MIMO configuration is used in the flat fading channel. The timing detection metric reported in [13] takes the shape of a triangular pulse at the double correlation detector, whereas a maximum of

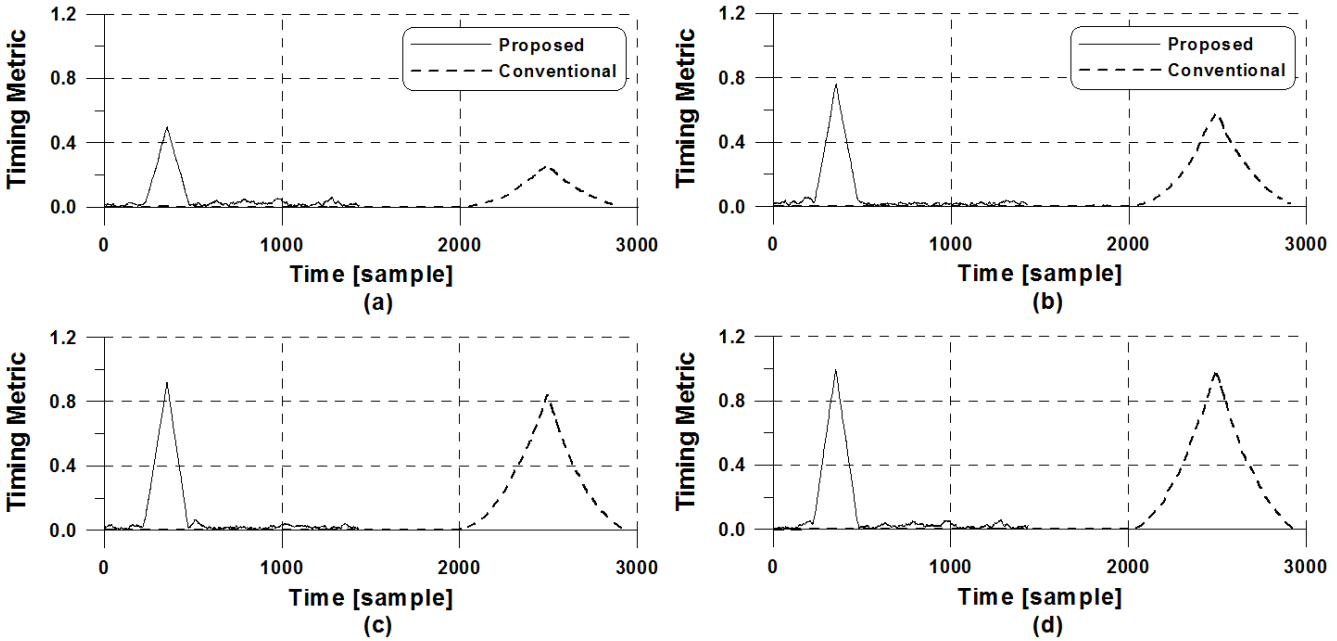

FIGURE 3. Timing detection metric in the flat fading channel: (a) SNR = 0dB (b) SNR = 5dB (c) SNR = 10dB (d) SNR = 30dB.

the correlation with quadratic decaying feature is detected in [14] and [15]. As illustrated in Fig. 3, the timing detection metric of the proposed scheme benefiting from the use of decimated correlation is more sharper than that of the existing algorithm [14], [15], which helps it to reliably detect the beginning of the P1 symbol.

B. JOINT FINE SYMBOL TIMING AND CFO ESTIMATION

Once $\hat{\delta}$ is obtained as formulated in (19), there still remains the estimation error $\zeta = \hat{\delta} - \delta$. Since the correlation outputs at each receive antenna are decimated by a factor of N_r at the initial phase, the correct arrival time point of an incoming T2-frame can be, with a high probability, positioned in the region $\mathcal{D} = \{-N_r \leq \zeta < N_r\}$. In order to obtain a more accurate estimation, $2N_r$ timing candidates for the correct arrival time are exhaustively examined during the second step. Bearing in mind the structure of the power-normalized correlation in (10), the correlation for the $2N_r$ candidates is defined as

$$\bar{C}_i(\hat{\delta} - d) = \frac{1}{P_c^i(\hat{\delta} - d)} \sum_{m=1}^{N_r} \left| C_m^i(\hat{\delta} - d, \epsilon) \right|, \quad i = 1, 2 \tag{20}$$

where $d \in \mathcal{D}$ is the trial value of ζ to match the offset. The timing candidates are then checked for acquiring the fine STO and CFO in a joint way. As a result, (12) and (20) are used for fine STO and CFO estimation:

$$\hat{\zeta} = \arg \max_{d \in \mathcal{D}} \left\{ \Omega_c(\hat{\delta} - d) \right\} \tag{21}$$

and

$$\hat{\epsilon} = \arg \left\{ \sum_{m=1}^{N_r} \sum_{i=1}^{2} C_m^i(\hat{\zeta}, \epsilon) \right\}. \tag{22}$$

One can easily see that the performance of (14) and (22) is equal if the symbol timing is perfectly estimated.

C. COMPLEXITY

For fair comparison, we define computational complexity of the symbol timing estimation schemes as the number of real floating point operations (flops) needed to complete each estimation. We count a complex multiplication as six flops, whereas a complex addition is counted as two flops [22]. Implementing $C_m^i(g, \epsilon)$ and $P_c^i(g)$ in (10) for $m = 1, 2, \cdots, N_r$ and $i = 1, 2$ needs $8(N_1 + N_2) \times N_r - 4N_r$ and $7(N_1 + N_2) \times N_r - 2N_r$ flops, respectively, whereas additional $2N_r$ flops are required to calculate the power-normalized correlation $\bar{C}_i(g)$. Finally, one flop is further demanded to compute the timing detection metric $\Omega_c(g)$. For each output sample, the total computational complexity consumed in the conventional estimation method is $N_{fc} = 15(N_1 + N_2) \times N_r - 4N_r + 1$. This search process in (13) is repeated over the T2-frame length L_f so that the total complexity of the conventional symbol timing estimation scheme can be formulated by $N_{fc} \times L_f$. Note that the minimum value for the T2-frame length is $L_f = 25$k samples when considering 1k FFT mode. In the proposed approach, formulating $D_m^i(g, \epsilon)$ and $Q_m(g)$ in (16) for $m = 1, 2, \cdots, N_r$ and $i = 1, 2$ needs $8(N_1 + N_2) - 4$ and $7(N_1 + N_2) - 2$ flops, respectively, whereas $3N_r$ extra flops are required to compute the overall correlation $\bar{D}_m(g)$. Finally, $N_r - 1$ flops are required to compute the

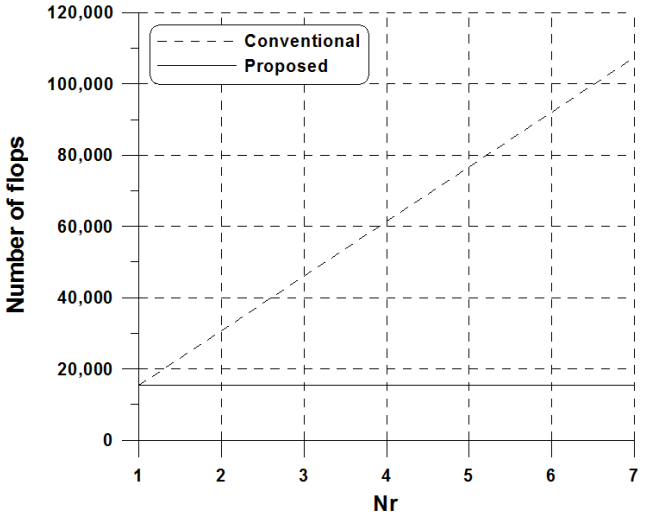

FIGURE 4. Complexity comparison between the proposed and conventional schemes.

timing detection metric $\Omega_p(g)$. The overall complexity of the proposed method used in the initial phase is $N_{fp1} = 15(N_1 + N_2) + 4N_r - 7$ for each output sample. At the second stage, $N_{fp2} = 2\,N_{fc} \times N_r$ extra flops are demanded to compute (20) and (21). Therefore, the total flops of the proposed symbol timing estimation method is counted by $N_{fp1} \times L_f + N_{fp2}$.

Figure 4 shows the computational complexity of the proposed and conventional schemes when $L_f = 25$k. For a simple illustration, we consider the number of flops normalized by L_f . It is evident that the complexity gap between the proposed and conventional schemes becomes more significant with larger N_r.

V. SIMULATION RESULTS

In order to verify the usefulness of the proposed synchronization algorithm, the simulations are conducted on 8MHz baseband DVB-T2 system with 1k normal OFDM symbols and a guard interval of 1/32 [4], taking into consideration $N_1 = 542$, $N_2 = 482$, $N_a = 1024$, and a center frequency of 600MHz. The performances of the existing and proposed estimation algorithms are compared in terms of both computational complexity and their performance. Table 1 lists up the channel models considered in our simulations [23], [24], whose normalized mean power is unity. A normalized CFO ϵ uniformly distributed in the range [0, 0.5] is considered, i.e. up to half of the subcarrier spacing of the DVB-T2 system. In the sequel, the conventional scheme adopts the timing detection metric corresponding to (12).

TABLE 1. Channel profiles.

No	Profile Name	Number of taps	Maximum delay (μs)
CM1	Rural area	4	0.6
CM2	Typical urban	6	5
CM3	Hilly terrain	6	17.2
CM4	Hellsinki	8	8.109

Figure 5 shows the mean square error (MSE) performance of the timing detection methods when 2×2 MIMO configuration is used. In this example, to restrict our attention to the performance comparison between the conventional and proposed schemes, the minimum value for the T2-frame length is considered so that $L_f = 25$k samples for 1k FFT mode. Irrespective of channel conditions, the MSE of the proposed estimation scheme is lower than that of the conventional estimation scheme. Since the side lobe of the timing detection metric is reduced as previously observed in Fig. 3, the proposed scheme achieves much better estimation over frequency-selective fading channels. Regarding the number of flops, the complexity of the proposed estimation scheme is significantly decreased by 50% in comparison with that of

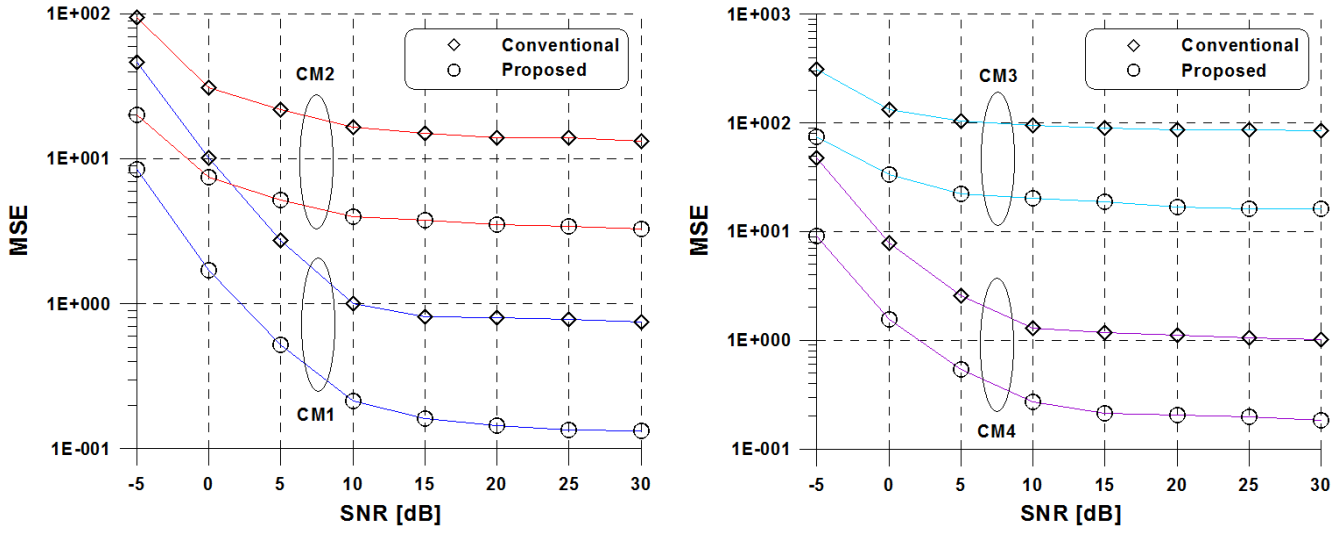

FIGURE 5. MSE of the symbol timing estimation schemes for 2×2 MIMO.

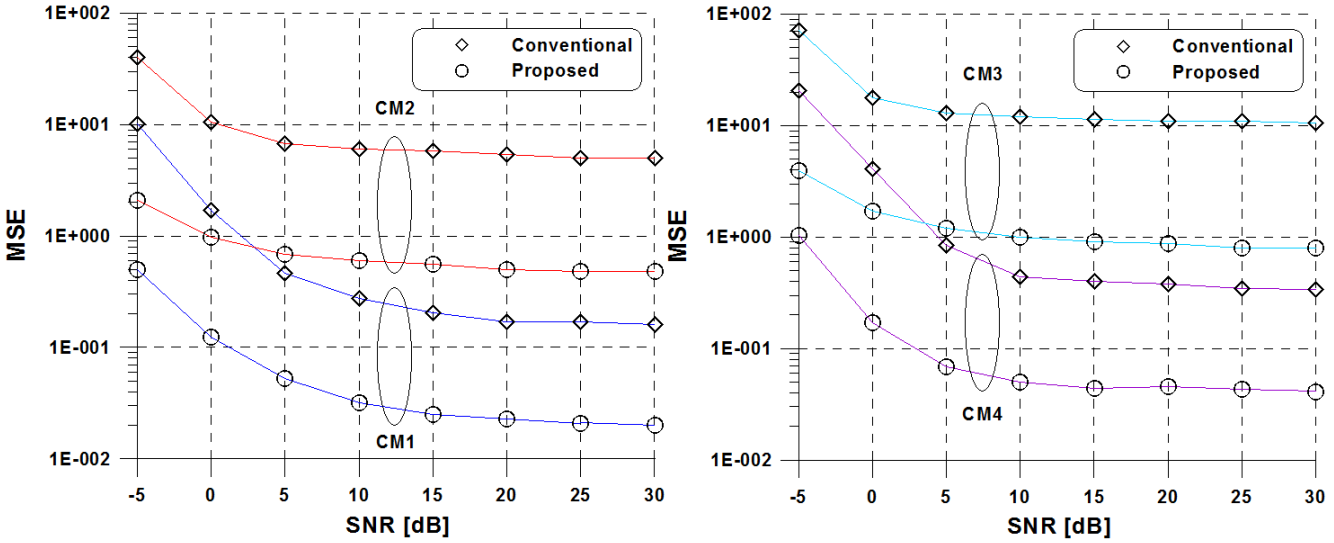

FIGURE 6. MSE of the symbol timing estimation schemes for 2 × 4 MIMO.

the existing estimation scheme considering 1k FFT mode and 2×2 MIMO configuration.

In Fig. 6, the MSE performance of the symbol timing detection schemes for 2×4 MIMO configuration is depicted under the same conditions as in Fig. 5. The relative performance of the conventional and proposed estimation methods is shown to be similar to that discussed in Fig. 5. As expected, the diversity gain can be improved with the increase in the number of receive antenna. Moreover, there is still a chance for additionally easing the computational complexity by increasing N_r at the cost of the performance gap between the both estimation schemes. When $N_r = 4$ and $L_f = 25$k, for example, a considerable complexity saving of 75% over the conventional estimation scheme can be achieved.

VI. CONCLUSION

This paper studied the the symbol timing issue for the OFDM-based DVB-T2 system with multiple antennas. The symbol timing synchronization scheme was proposed to aim at enhancing the estimation accuracy as well as designing its simple receiver structure. To this end, a new timing detection metric that improves the performance of the P1 symbol timing synchronization was presented in the MIMO DVB-T2 system. Our simulation results have shown that such a design achieves not only a low computational cost but also a superior performance compared to the conventional estimation scheme.

REFERENCES

[1] *Radio Broadcasting Systems: Digital Audio Broadcasting (DAB) to Mobile, Portable and Fixed Receivers*, document ETSI ETS 300 401, ETSI, Sophia Antipolis, France, Jun. 2006.
[2] *Digital Video Broadcasting (DVB): Frame Structure, Channel Coding and Modulation for Digital Terrestrial Television (DVB-T)*, document ETSI ETS 300 744, ETSI, Sophia Antipolis, France, Jan. 2009.
[3] *Digital Radio Mondiale (DRM)—System Specification*, document ETSI ES 201 980 V3.1.1, Jan. 2014.
[4] *Frame Structure Channel Coding and Modulation for a Second Generation Digital Terrestrial Television Broadcasting System (DVB-T2)*, document ETSI EN 302 755 V.1.4.1, Jul. 2015.
[5] *Digital Video Broadcasting, Next Generation Broadcasting System to Handheld, Physical Layer Specification (DVB-NGH)*, document A160, DVB, 2012.
[6] M. S. Hossen, S.-H. Kim, and K.-D. Kim, "Stereoscopic video transmission over DVB-T2 system using future extension frame," *IEEE Trans. Broadcast.*, vol. 62, no. 4, pp. 817–825, Dec. 2016.
[7] Z. Kui *et al.*, "Advanced preamble transmit diversity of polarized DVB-T2 MISO system using hybrid differential modulation," *IEEE Trans. Broadcast.*, vol. 61, no. 4, pp. 723–728, Dec. 2015.
[8] J. H. Seo, T. J. Jung, H. M. Kim, and D. S. Han, "Improved polarized 2×2 MIMO spatial multiplexing method for DVB-NGH system," *IEEE Trans. Broadcast.*, vol. 61, no. 4, pp. 729–733, Dec. 2015.
[9] *Channel Coding, Frame Structure and Modulation Scheme for Terrestrial Integrated Service Digital Broadcasting (ISDB-T)*, document ITU-R. WP 11A/59, 1999.
[10] *ATSC Standard: Physical Layer Protocol*, document A/322, Jun. 2017.
[11] D. Gómez-Barquero *et al.*, "MIMO for ATSC 3.0," *IEEE Trans. Broadcast.*, vol. 62, no. 1, pp. 298–305, Mar. 2016.
[12] *Implementation Guidelines for a Second Generation Digital Terrestrial Television Broadcasting System (DVB-T2)*, document ETSI TS 102 831 V1.2.1, Aug. 2012.
[13] J. G. Doblado, V. Baena, A. C. Oria, D. Perez-Calderon, and P. Lopez, "Coarse time synchronisation for DVB-T2," *Electron. Lett.*, vol. 46, no. 11, pp. 797–799, May 2010.
[14] A. Vießmann *et al.*, "Implementation-friendly synchronisation algorithm for DVB-T2," *Electron. Lett.*, vol. 46, no. 4, pp. 282–283, Feb. 2010.
[15] D. H. Sayed, M. Elsabrouty, and A. F. Shalash, "Improved synchronization, channel estimation, and simplified LDPC decoding for the physical layer of the DVB-T2 receiver," *EURASIP J. Wireless Commun. Netw.*, vol. 2013, Mar. 2013, Art. no. 60.
[16] A. A. Nasir, S. Durrani, and R. A. Kennedy, "Performance of coarse and fine timing synchronization in OFDM receivers," in *Proc. ICFCC*, vol. 2, May 2010, pp. 412–416.
[17] L. Nasraoui, L. N. Atallah, and M. Siala, "An efficient reduced-complexity two-stage differential sliding correlation approach for OFDM synchronization in the AWGN channel," in *Proc. Veh. Technol. Conf. (VTC Fall)*, Dec. 2011, pp. 1–5.
[18] X. Zhang, H. Bie, C. Lei, and J. Zheng, "A robust timing and frequency synchronization scheme for DVB-T2 system," in *Proc. Veh. Technol. Conf. (VTC Spring)*, May 2015, pp. 1–6.
[19] Y. Yao and G. B. Giannakis, "Blind carrier frequency offset estimation in SISO, MIMO, and multiuser OFDM systems," *IEEE Trans. Commun.*, vol. 53, no. 1, pp. 173–183, Jan. 2005.

[20] S. Salari and M. Heydarzadeh, "Joint maximum-likelihood estimation of frequency offset and channel coefficients in multiple-input multiple-output orthogonal frequency-division multiplexing systems with timing ambiguity," *IET Commun.*, vol. 5, no. 14, pp. 1964–1970, Sep. 2011.
[21] T.-T. Lin and F.-H. Hwang, "On the CFO/Channel estimation technique for MIMO-OFDM systems without using a prior knowledge of channel length," *EURASIP J. Wireless Commun. Netw.*, vol. 2015, Dec. 2015, Art. no. 79.
[22] G. H. Golub and C. F. Van Loan, *Matrix Computations*, 3rd ed. Baltimore, MD, USA: The Johns Hopkins Univ. Press, 1996.
[23] M. Failli, "Digital land mobile radio communications-COST 207," Commission Eur. Community, Final Rep., 1989.
[24] M. Petrov *et al.*, "Configuration for multi-path MIMO channel simulations in NGH," DVB Tech. Module Sub-Group Next Gener. Handheld, Tech. Rep. TM-NGH641r8, Feb. 2011.

YONG-AN JUNG received the B.S. and M.S. degrees from the Department of Computer Engineering, Sejong University, Seoul, South Korea, in 2011 and 2013, respectively, where he is currently pursuing the Ph.D. degree with the School of Computer Engineering.

His research interests are in the areas of wireless/wired communications systems design, spread spectrum transceivers, and system architecture especially for realizing advanced orthogonal frequency-division multiplexing communications systems.

HYOUNG-KYU SONG received the B.S., M.S., and Ph.D. degrees in electronic engineering from Yonsei University, Seoul, South Korea, in 1990, 1992, and 1996, respectively.

From 1996 to 2000, he was a Managerial Engineer with the Korea Electronics Technology Institute, Gyeonggi-do, South Korea. Since 2000, he has been a Professor with the Department of Information and Communication Engineering, Sejong University, Seoul. His research interests include digital and data communications, and information theory and their applications with an emphasis on mobile communications.

YOUNG-HWAN YOU received the B.S., M.S., and Ph.D. degrees in electronic engineering from Yonsei University, Seoul, South Korea, in 1993, 1995, and 1999, respectively.

From 1999 to 2002, he was a Senior Researcher with the Wireless Pan Technology Project Office, Korea Electronics Technology Institute, South Korea. Since 2002, he has been an Associate Professor with the Department of Computer Engineering, Sejong University, Seoul. His research interests lie in the field of wireless communications and signal processing, with a focus on wireless/wired communications systems design, spread spectrum transceivers, and system architecture for realizing advanced digital communications systems, especially, for wireless orthogonal frequency-division multiplexing.